A Low Profile Circularly Polarized Antenna based on Stepped Open-ended Slot Radiator

Ping Wang [1], Qi Wu [1], Yu Shao [1], and Dong Huang [2]

[1] School of Communications and Information Engineering
Chongqing University Posts and Telecommunications, Chongqing, 400065, China
wp@cqupt.edu.cn, 641837048@qq.com, shaoyu@cqupt.edu.cn

[2] Chongqing Institute of Green and Intelligent Technology
Chinese Academy of Sciences, 400714, China
chenyijia000011@163.com

Abstract ─ A compact wide band and low profile circularly polarized antenna is presented based on stepped open-ended slotline in this paper. The antenna is composed of four open-end-slotted patches and a feed network. Four open-end-slotted patches are sequentially rotated and vertically soldered on the ground plane of the feed network, and are excited by a wide band transition from strip-line to slot-line with short pin in antenna element. The CP radiation of the proposed antenna is realized by four output ports of the feed network which transmit four signals that have equal amplitude with quadrature phase difference (0^0, 90^0, 180^0, and 270^0). Simulation results are compared with the measurements, and a good agreement is obtained. The measured results show that the proposed antenna can provide broad impedance bandwidth of 73.4% (3.5 GHz–7.56 GHz) (reflection coefficient less than -10 dB), a maximum gain of 4.74 dBi, and a 3-dB axial ratio (AR) bandwidth of about 35.1% (3.65 GHz–5.2 GHz).

Index Terms ─ Circularly polarized (CP) antenna, low profile, open-ended slotline, stepped slotline, feed network, wide band.

I. INTRODUCTION

Due to the unique features that circularly polarized (CP) antenna can increase orientation diversity and reduce the loss caused by the multi-path effects between transmitting and receiving antennas, CP antenna has been researched widely over the past decades. One most typical example of CP antenna is various shaped patch with a slight structure perturbation at a specific location to form two orthogonal linear polarizations with a 90^0 phase shift [1-3], but these antennas have inherent narrow impedance and axial ratio (AR) bandwidth (typically 1%-4%). In order to enhance the bandwidth, commonly one method is the use of parasitic elements [4-9]. In [4], a design realizes the circularly polarized performance using a stacked arrangement of the corner-truncated rectangular patch, where AR bandwidth of better than 11% and impedance bandwidth of better than 27% were obtained. In [5], a micro-strip-fed hexagonal patch with a slant slot-line is proposed for CP application, where a parasitic element with different size was introduced to broaden 3dB AR bandwidth to 5%. Fang et al. investigated the cut-corner stacked path antenna, in which a horizontally meandered strip (HMS) feed technique is proposed to obtain impedance bandwidth of 25.8% and 3-dB AR bandwidth of 13.5% for universal ultrahigh frequency (UHF) RF identification applications [6]. A hybrid combination of coupling feed technique and parasitic element was also introduced to achieve larger 3dB AR bandwidth, such as slot coupling (2.8%) [7], T-shaped strip coupling (0.98%, 4.275%, 0.8869%, and 1.35% in four distinct bands) [8], and L-shaped strip coupling (10%) [9, 10]. However, the aperture coupled antenna needs a reflecting plate to block back radiation, which increases the complexity of the antenna configuration. In addition, the effects of the length of the vertical and horizontal portion of the L-shaped or T-shaped strip on input resistance and reactance are dependent, which result in complex design process. It is seen that though the antennas have a low profile structure, the AR bandwidth is still very narrow.

Another example of CP antenna is the sequentially multi-fed-rotated CP antenna presented in [11-15], in which generally a hybrid feed network need be designed to provide a relative phase shift of 90 degree and equal amplitude in the output port. In [11], a 2×2 circularly polarized stacked patch array was proposed, but only 12% impedance and 8% 3dB AR bandwidths are achieved. Single radiation patch fed by a complex feed network without 100Ω isolation resistor to realize a high gain and wide axial ratio beam-widths was also presented in [12], whereas only 11% AR bandwidth is achieved owing to the narrow band characteristic of single patch. In [13],

Shen et al. presented a low profile CP antenna based on quarter-mode substrate integrated wave guide, but the antenna provides the only 5.8% AR bandwidth. It is important to note that a circularly polarized antenna array based on anti-podal Vivaldi antenna was proposed, and exhibits 10-dB return loss and 3-dB AR bandwidths from 1 GHz to 10 GHz [14]. However, its size is too large, especially in profile size of 173 mm. A size reduction based on halved Vivaldi antenna is also presented in [15], but the profile size of $0.42 \lambda_L$ (λ_L is the free-space wavelength at the center frequency) is still large for some wireless communication systems.

In this paper, we present a wide band and low profile circularly polarized antenna with a profile size of only $0.19 \lambda_L$ (λ_L is the free-space wavelength corresponding to lowest operating frequency).The antenna is formed by four sequentially rotated rectangle patches with open-ended slot-line, and is fed by using four output ports of feed network to realize the CP performance. The antenna is studied using the package ANSYS high-frequency structure simulator (HFSS), which is based on the finite element method. An antenna prototype is fabricated and measured to verify the simulation and findings.

II. PROPOSED ANTENNA CONFIGURATION AND DISCUSSION

Figure 1 shows the geometry of the overall CP antenna prototype. In this design, an FR-4 substrate (dielectric constant = 4.4, loss tangent = 0.02) with a thickness of 0.8 mm was employed as the system circuit board and the overall dimension is about 60 mm×60 mm. A system ground plane with a same size is printed on the top layer of the substrate, whereas the feed network resides on the bottom layer of the substrate. The feed network is composed by the Wilkinson power divider, 90 degree delay line, and 180 degree delay lines, and brings into sequential rotation of current on the radiation patch for CP radiation. One end of the 50-Ω feeding strip-line is connected to the inner conductor of a 50-Ω SMA connector for testing the antenna, while the other end is connected to the Wilkinson power divider. The external metal shell of the SMA connector is soldered to the system ground plane.

Four rectangle-supported substrate boards, which also are fabricated by FR-4 substrate with a thickness of h=0.5 mm, are integrated together to form a hollow square-ring wall and are located on system ground plane vertically. Four rectangle patches are printed on four exterior face of the supported dielectric wall respectively and the bottom edge of that is soldered to the system ground plane, whereas three slot-lines with different slot widths are etched on each rectangle patch to form a stepped open-ended slot radiator. On the interior face of the supported dielectric wall, coupling micro-strip line is

printed and one end of that is extended to couple the stepped slot-line, and then is connected through the short circuit pins (E, F, G, H) to the rectangle patch. Other end of the coupling micro-strip line is connected to the output ports of the feed network that have equal amplitude with quadrature phase difference (0^0, 90^0, 180^0, and 270^0). It should be mentioned that to fix the rectangle-supported dielectric wall vertically on the system ground plane two tips on each substrate boards were deliberately made and inserted into the etched slot on system ground plane, and the existence of the tip slightly affects the resonant frequency and radiation patterns, which can be included in the full-wave simulation.
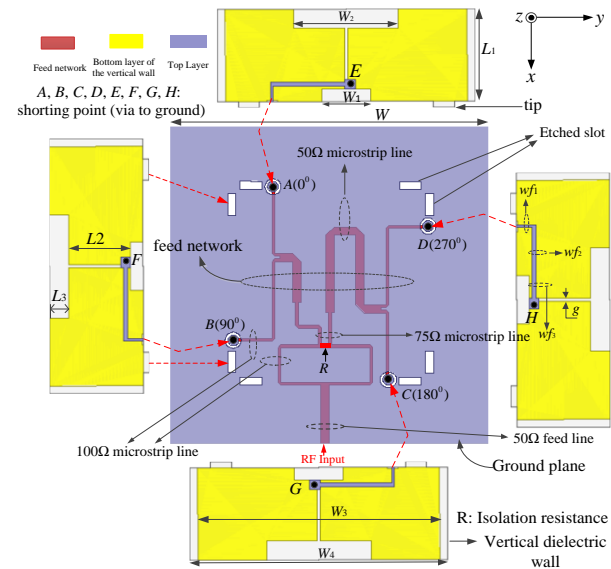

Fig. 1. Geometry and dimensions of the proposed antenna: W=60, w_1=7, w_2=15, w_3=36, w_4=37, wf_1=0.31, wf_2=0.67, wf_3=1.5, L_1=15, L_2=9.9, L_3=3.1. (Unit: mm).

To study the functions of the stepped configuration, the following cases, i.e., Ant 1(slot-line structure with metal wall and dielectric wall, which means that four rectangle patches encircle into a square ring wall successively), Ant 2 (stepped slot-line structure with metal wall and dielectric wall) and Ant 3 (stepped slot-line structure with dielectric wall and four separated rectangle patches) as shown in Fig. 2, are analyzed. The simulated results of |S11| of Ant 1, Ant 2 and Ant 3 are shown in Fig. 2. It is clear from the figure that Ant 1 produces wider impedance bandwidth owing to the extension of the effective current path on the metal wall formed by interconnected four rectangle patches, but the 3 dB AR bandwidth is poor. When the stepped slot-line structure is used in Ant 1, Ant 2 is formed. Although the impedance bandwidth is narrower, the axial ratio is improved. Ant 3 is formed by truncating the vertical edge of the rectangle patch in Ant 2, which shows that the

metal wall in Ant 2 is decomposed into four separated patches with same size. Because coupling between radiation patches is reduced, Ant 3 achieves better impedance bandwidth and 3 dB AR bandwidth, as shown in Fig. 2.

Figure 3 demonstrates the impact of varying the function of L_3 on the reflection coefficient of the antenna. The figure shows that when increasing L_3 the resonance band is shifted downward, and vice versa, i.e., the lowest working frequency is 3.82 GHz when $L_3=0$, the lowest working frequency is 3.65 GHz as the L_3 is added from 0 to 3.1 mm, and 3.37 GHz as L_3 is increased from 3.1 mm to 8.1 mm. Therefore, L_3 should be selected appropriately to compromise on good impedance matching and low profile requirement.
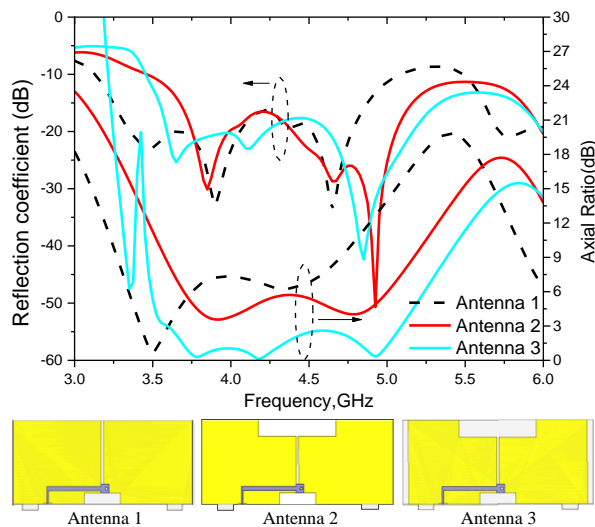

Fig. 2. Simulated reflection coefficient and axial ratio of Ant 1, Ant 2, and Ant 3.
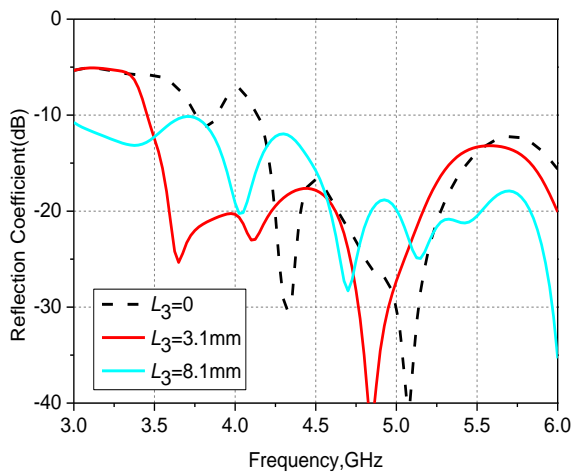

Fig. 3. Simulated reflection coefficient for the proposed antenna as a function of L_3.

Figure 4 shows the reflection coefficient and axial ratio performance versus frequency for different w_2 when other parameters are kept unchanged. It is clearly known from the figure that varying the parameter w_2 has less effect on impedance matching, whereas w_2 is increased from 5 mm to 20 mm, the AR bandwidth are slightly changed and three lowest AR values (f_1, f_2, f_3) are produced. It is also observed that with variety of w_2 results in significant shifts up of the first resonance (f_2), shifts downward of the second resonance (f_2), almost no change of third resonances (f_3). To have a wider and proper AR bandwidth, the parameter w_2 needs to be well optimized.
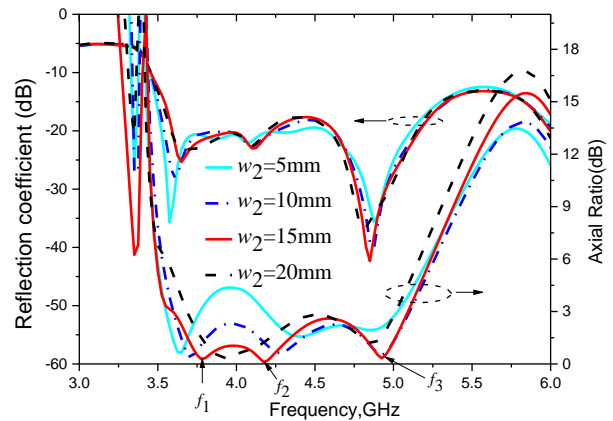

Fig. 4. Simulated reflection coefficient and axial ratio for the proposed antenna as a function of w_2.
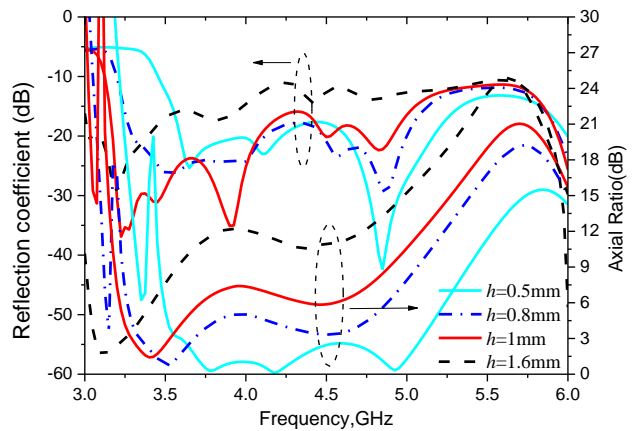

Fig. 5. Simulated reflection coefficient and axial ratio for the proposed antenna as a function of h.

The effect of the thickness of the supported dielectric wall (h) on reflection coefficient and axial ratio is illustrated in Fig. 5. It is found that the parameter h has large effect on the reflection coefficient and axial ratio. When the parameter h is increased, the curves of both reflection coefficient and axial ratio are shifted

downward, and the AR performance becomes worse. Results have revealed that the best performance is obtained when h=0.5 mm.

III. SIMULATED AND EXPERIMENTAL RESULTS

To verify the effectiveness of the design, a prototype of the proposed antenna with the dimensions shown in Fig. 1 was fabricated. A photograph of the fabricated antenna is displayed in Fig. 6 (a). The radiation performance of the antenna was measured in an anechoic chamber using the NSI300V-30X30 far-field measurement system and The VSWR results of the proposed antenna are measured using a calibrated Agilent vector network analyzer N5230A.
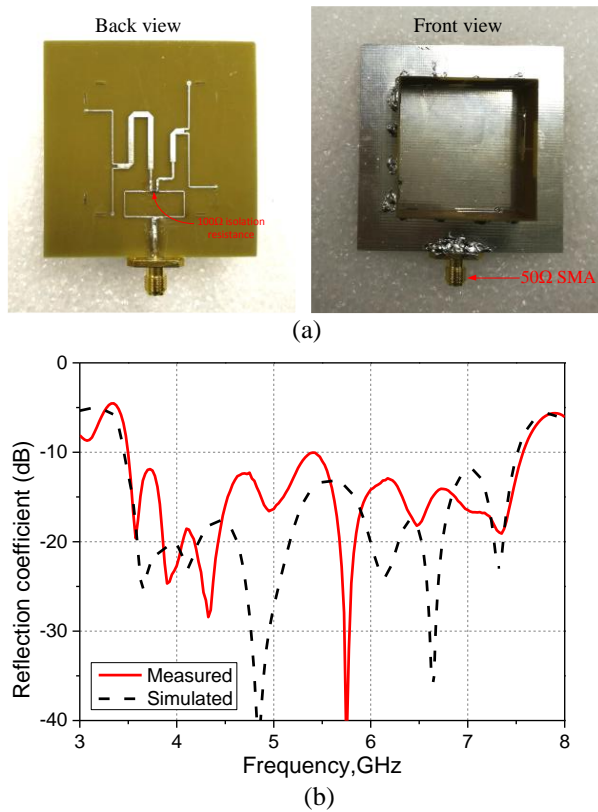

(a)

(b)

Fig. 6. (a) Fabricated antenna, and (b) comparison of simulated and measured reflection coefficient of the proposed antenna.

A. Reflection coefficient, axial ratio, and realized gain

Measured and simulated reflection coefficient for the proposed antenna are shown in Fig. 6 (b), which shows a little discrepancy due to the error of substrate parameters of the FR-4 substrate and tolerance in manufacturing. It is seen clearly that the measured reflection coefficient is less than -10 dB over the frequency ranges of 3.5 GHz–7.56 GHz (73.4%), which

is complied with simulated results. Figure 7 shows the comparison between the simulated and measured AR at broadside direction (+z). The measured 3-dB AR bandwidth of 3.65 GHz–5.2 GHz or 35.1% is obtained. Within the frequency range, the measured gain of the proposed antenna is 2.52 dBi on average and 4.27 dBi at maximum when the operating frequency is 5.2 GHz. A gain increased slightly over the operating band is found experimentally.

B. Radiation pattern

Figure 8 shows the comparison between the simulated and measured radiation patterns at 3.8 GHz, 4.2 GHz, and 4.95 GHz, in the xz-plane and yz-plane, respectively. It is seen that the proposed antenna radiates a right-hand circular polarization (RHCP), and has an approximately symmetrical radiation pattern across the operating bandwidth. The symmetrical radiation pattern should be attributed to the square ring-shaped radiator and system ground plane, whereas the back lobe and cross-polarization (left-hand circular polarization, LHCP) components are unsymmetrical in the working bands due to the effect of parasitical radiation of feed network and edge diffraction of compact ground plane. The measured and the simulated results of the RHCP radiation pattern are in good agreement, and its maximum beam is always directed to the +z-axis direction, which have great advantages in practical applications.
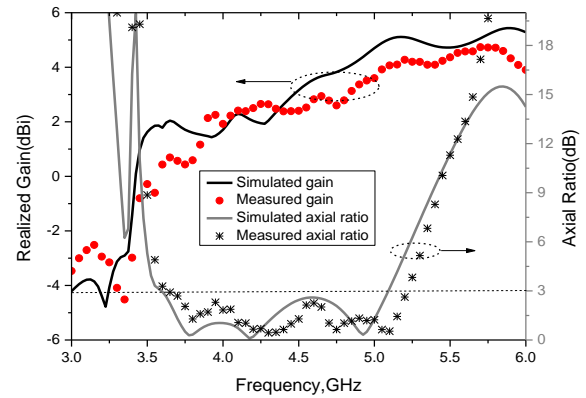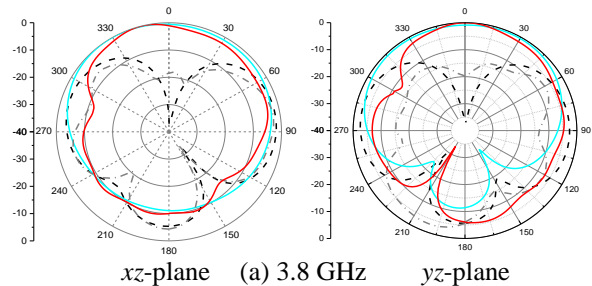

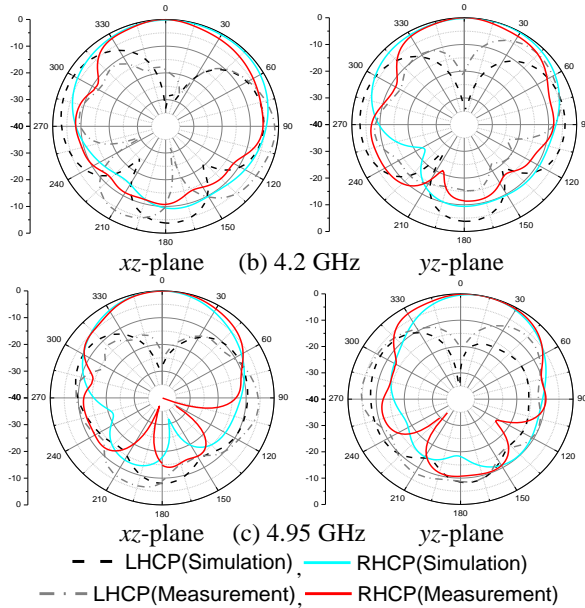Fig. 7. Simulated and measured peak realized gain and axial ratio.

xz-plane   (a) 3.8 GHz yz-plane

Fig. 8. Normalized radiation patterns at three resonant frequencies: (a) 3.8 GHz, (b) 4.2 GHz, and (c) 4.95 GHz.

C. Performance comparison

The performance of the proposed antenna is compared with previous designs in the literature in terms of fractional bandwidth, AR bandwidth, profile size, gain, as shown in Table 1. It is seen that our proposed antenna has the widest impedance bandwidth, while maintaining a low profile. More importantly, the designed antenna also shows good circularly polarized characteristics. From comprehensive view, our antenna is suitable for practical application environments. The design in [5] has a small AR bandwidth, though its profile is smaller than that of our antenna. The antenna in [12], constructed by using square patch, uses a four-feed network to equal amplitude and quadrature phase difference, while its bandwidth is still smaller a than that of our proposed antenna. The design in [13] has a very impressive low profile, though its bandwidth is very small, only 5.8%. Based on Vivaldi antenna structure, a wideband circularly polarized antenna is proposed in [15], but the profile size of $0.42\lambda_L$ is larger than that of our antenna. Compared with the works in [16, 17], our proposed antenna exhibits larger bandwidth.

Table 1: Performance comparison between the proposed antenna and other reported CP antennas

Reference	VSWR	Lowest Operating Frequency (λ_L is Referencing Wavelength)	Impedance Bandwidth	AR Bandwidth	Profile Size (mm)	Gain (dBi)
[5]	<2	1.54 GHz (194.8 mm)	11%	5%	24.8 ($0.127\lambda_L$)	>6.5
[12]	<1.5	0.86 GHz (348.8 mm)	19.7%	11%	34 ($0.097\lambda_L$)	8.36~9.65
[13]	<2	5.02 GHz (59.76 mm)	8.4%	5.8%	2.84 ($0.048\lambda_L$)	~5.58
[15]	<2	3.45 GHz (86.95 mm)	57.3%	41.4%	36.8 ($0.42\lambda_L$)	>6.9
[16]	<2	2.8 GHz (107.1 mm)	34%	34%	1.6 ($0.02\lambda_L$))	5.3~7.5
[17]	<2	3.45 GHz (86.95 mm)	13.5%	8%	1.6 ($0.02\lambda_L$))	4~7.8
This work	<2	3.65 GHz (82.2 mm)	73.4%	35.1%	15.5 ($0.19\lambda_L$)	0.69~4.74

IV. CONCLUSION

A low profile circularly polarized antenna based on stepped open-ended slot radiator has been presented in this paper. The antenna is formed by sequentially rotating four isolated rectangle patches with stepped slot-line, and encircle into a square ring structure, then is located vertically on a square ground plane. To realize broadband CP performance, Wilkinson power dividers, 90 degree delay line, and 180 degree delay lines are used to form a feed network of four output ports with a relative phase shift of 90 degree and equal amplitude, in which each output port is sequentially connected to the coupling micro-strip line on the interior face of the vertical dielectric wall. The optimized antenna has achieved a broad impedance bandwidth of 73.4% (3.5 GHz–7.56 GHz) (reflection coefficient less than -10 dB), a maximum gain of 4.74 dBi, and a 3-dB axial ratio (AR) bandwidth of about 35.1% (3.65 GHz–5.2 GHz). Moreover, the antenna is compact and its profile size is only about 0.19λ. The results indicate that the proposed antenna is an excellent candidate for various wireless systems.

Education Committee (No. KJ1600409).

REFERENCES

[1] I. Taha, K. Ayyuce, and S. ismail, "Circularly polarized microstrip patch antenna slits,"*Appl. Comp. Electromagnetics Society (ACES) Conference*, EM Simulations Using Sonnet-I, 2010.

[2] Nasimuddin, Z. N. Chen, and X. M. Qing, "Asymmetric-circular shaped slotted microstrip antennas for circular polarization and RFID applications," *IEEE Trans. Antennas Propag.*, vol. 58, no. 12, pp. 3821-3828, 2010.

[3] K. F. Tong and T. P. Wong, "Circularly polarized U-slot antenna," *IEEE Trans. Antennas Propag.*, vol. 55, no. 8, pp. 2382-2385, 2007.

[4] S. Shekhawat, P. Sekra, D. Bhatnagar, V. K. Saxena, and J. S. Saini, "Stacked arrangement of rectangular microstrip patches for circularly polarized broadband performance," *IEEE Trans. Wireless Propag. Lett.*, vol. 9, pp. 910-913, 2010.

[5] T. Mondal, S. Samanta, R. Ghatak, and S. R. B. Chaudhuri, "A novel hexagonal wideband circularly polarized stacked patch microstrip antenna," *Microwave Opt. Technol. Lett.*, vol. 57, no. 11, pp. 2548-2554, 2015.

[6] Z. B. Wang, S. J. Fang, S. Q. Fu, and S. L. Jia, "Single-fed broadband circularly polarized stacked patch antenna with horizontally meandered strip for universal UHF RFID applications," *IEEE Trans. Microw. Theory Tech.*, vol. 59, no. 4, pp. 1066-1073, 2011.

[7] A. R. Weily and N. Nikolic, "Circularly polarized stacked patch antenna with perpendicular feed substrate," *IEEE Trans. Antennas Propag.*, vol. 61, no. 10, pp. 5274-5278, 2013.

[8] D. K. Singh, B. K. Kanaujia, S. Dwari, G. P. Pandey, and S. Kumar, "Novel quad-band circularly polarized capacitive-fed microstrip antenna for C-band applications," *Microwave Opt. Technol. Lett.*, vol. 57, no. 11, pp. 2622-2628, 2015.

[9] S. L. S. Yang and K. M. Luk, "A wideband L-probes fed circularly-polarized reconfigurable microstrip patch antenna," *IEEE Trans. Antennas Propag.*, vol. 56, no. 2, pp. 581-584, 2008.

[10] K. M. Luk, K. F. Lee, and H. W. Lai, "Development of wideband L-probe coupled patch antenna,"*Appl. Comp. Electromagnetics Society (ACES) Journal*, vol. 22, no. 1, pp. 620-625, 2007.

[11] A. Kumar and M. V. Kartikeyan, "A circularly polarized stacked patch aperture coupled microstrip antenna for 2.6GHz band," *Int. J. Infrared Milli. Waves*, vol. 28, no. 1, pp. 13-23, 2007.

[12] P. Wang, G. Wen, J. Li, Y. Huang, L. Yang, and Q. Zhang, "Wideband circularly polarized UHF RFID reader antenna with high gain and wide axial ratio beamwidths," *Prog. Electromagn. Res.*, vol. 129, pp. 65-385, 2012.

[13] C. Jin, Z. X. Shen, R. Li, and A. Alphones, "Compact circularly polarized antenna based on quarter-mode substrate integrated waveguide subarray," *IEEE Trans. Antennas Propag.*, vol. 62, no. 2, pp. 963-967, 2014.

[14] K. K. M. Chan, A. E. C. Tan, and K. Rambabu, "Decade bandwidth circularly polarized antenna array," *IEEE Trans. Antennas Propag.*, vol. 61, no. 11, pp. 5435-5443, 2013.

[15] Y. J. Hu, Z. M. Qiu, B. Yang, S. J. Shi, and J. J. Yang, "Design of novel wideband circularly polarized antenna based on Vivaldi antenna structure," *IEEE Trans. Wireless Propag. Lett.*, vol. 14, pp. 1662-1665, 2015.

[16] M. H. Rasekhmanesh, A. Piroutiniya, and P. Mohammadi, "Wideband circularly polarized antenna array using sequential phase feed structure and U-shape radiating patch elements for S-band applications," *Microwave Opt. Technol. Lett.*, vol. 59, no. 11, pp. 2806-2812, 2017.

[17] M. H. Rasekhmanesh, P. Mohammadi, and A. Piroutiniya, "A circularly polarized miniaturized array using combination of circle and rectangular lines in the sequential phase feed structure," *Appl. Comp. Electromagnetics Society (ACES) Journal*, vol. 32, no. 4, pp. 339-343, 2017.

Ping Wang was born in Chongqing, China. He received his M.S. degree in Theoretical Physics from Chongqing University of China in 2008 and the Ph.D. degree in University of Electronic Science and Technology of China (UESTC) in 2013, respectively. Currently, he is working in Chongqing University of Posts and Telecommunications, China. His current research interests include patch antennas, wide band antennas, and arrays.

Qi Wu, master degree candidate of Chongqing University of Posts and Telecommunications. His main research direction is circularly polarized antenna, tag antenna, end-fire antenna, metamaterial, and electromagnetic theory and application in communication.

Yu Shao was born in Kunming, Yunnan Province, China. He received his M.Eng. degree in Electromagnetic Field and Microwave Technology from Wuhan University, Wuhan, China, in 2009 and the Ph.D. degree in Electrical Engineering from Auburn University, USA, in 2015. Currently, he is working in Chongqing University of Posts and Telecommunications, China. His research interests include computational electromagnetics, antennas and bio-electromagnetics.

Dong Huang was born in Chongqing, China. He currently is working in Chongqing Institute of Green and Intelligent Technology, Chinese Academy of Sciences, China. His research interests include computational electromagnetics, antennas and wireless communications.